Indian Journal of Fibre & Textile Research
Vol. 33, December 2008, pp. 383-387

A method for validation of a model of balloon in ring frame

Milan Sharma & Anirban Guha[a]
Department of Mechanical Engineering, Indian Institute of Technology, Mumbai 400 076, India

Received 26 November 2007; revised received and accepted 16 May 2008

A novel approach has been presented for validating the models developed for predicting the shape of the ring yarn balloon. The initial conditions have been obtained from the experimental data, i.e. images of yarn balloon. The differential equations have been solved by Euler Cauchy numerical method. The resulting balloon shapes predicted by the model are found to be quite different from the actual balloon shapes.

Keywords: Balloon envelope, Ring frame, Yarn balloon

IPC Code: Int. Cl.[8] G05B17/00

1 Introduction

Accurate modelling of the balloon formed by yarn during ring spinning will provide a better insight into the mechanics of ballooning and the parameters influencing it. This may aid in design of better systems for controlling the balloon. Therefore, a number of researchers have attempted to model the ring frame balloon. The monograph by DeBarr and Catling[1] reports the study of many others on this subject. More recent work has advanced the theory, a few of them being the work of Batra *et al*.[2-4], Ghosh *et al*.[5], Zhu *et al*.[6] and Sharma and Rahn[7]. All these models require some parameters and initial conditions to be obtained from experimental data. The approach by Batra *et al*.[2] was inspired by the fact that non-dimensionalizations in the earlier formulations yielded parameters that were difficult to relate to physical parameters of the yarn balloon. The approach proposed by them has been further developed in their latter papers.[3-5]

The success of a model can be judged by comparing the results predicted by the model with experimental data. In this case, experimental data would be in the form of images of yarn balloon during the operation of a ring frame. These would have to be compared with the balloon shape predicted by the model. This exercise has been reported by Batra *et al*.[4], Zhu *et al*.[6] and Sharma and Rahn[7]. In the paper by Batra *et al*.[4], bifurcation theory[8] has been used to obtain a solution of the set of nonlinear ordinary differential equations which can describe the motion of a yarn through a ring spinning system. For the prediction of the shape of the yarn balloon, the spinning tension was calculated by assuming certain values for yarn-traveller and ring-traveller coefficients of friction and air drag coefficient. Zhu *et al*.[6] and Sharma and Rahn[7] have used a model based on the approach of Perkins and Mote[9]. However, the nonlinear differential equations derived by them have been solved by choosing the initial conditions so that the error is minimised. A root finding algorithm implemented in Matlab has been used for this purpose. A better test of any mathematical model would be to determine the initial conditions from experimental data. The present work therefore represents a new approach in validating a mathematical model of a ring yarn balloon where the initial conditions have been obtained from experimental data. The model proposed by Batra *et al*.[3] has been chosen for this purpose. The spinning tension has been experimentally determined. Images of yarn balloon in ring frame under varying condition have been captured and compared with the balloon shapes predicted by the model. The initial conditions and various process dependent parameters have been derived from the same balloon images. The method of verification of a ring frame balloon model proposed here is not limited to model used in this work. It can be extended to the models proposed by other authors too.

[a]To whom all the correspondence should be addressed.
E-mail: anirbanguha@yahoo.com

2 Materials and Methods

Two yarns (one white and one red), each of 33.5 tex, were fed through the pair of front rollers of a ring frame. They were wound on a bobbin in the same way as a yarn is spun with a twist of 848 tpm. Photographs of yarn balloon in ring frame were captured by varying the following parameters: (i) height of the balloon (h) —250, 190 and 140mm; (ii) spindle speed — 7000, 12000 and 16000rpm; and (iii) traveller mass — 37.1, 27.8 and 18.7mg.

The height of the balloon was assumed to be equal to the vertical distance between lappet guide and ring. The speed of the traveller was assumed to be equal to the spindle since the difference was only about 2%. Out of these 27 experiments, the balloon showed a propensity for collapsing frequently in eight cases. At least 10 photographs were taken for each of the 19 experiments which could be conducted successfully. The photographs were taken with a shutter speed of 1/400 s. This meant that the yarn was able to make 0.29, 0.5 and 0.67 revolutions during the time of exposure, corresponding to the three different spindle speeds. This ensured that even for the 7000 rpm experiments, a few of the 10 photographs would show the balloon envelope on one side of the spindle.

3 Results and Discussion

3.1 The Model

The model proposed by Batra *et al.*[3] assumes the following:

(i) The yarn is assumed to be uniform with a constant linear density.

(ii) The guide eye is assumed to be a point constraint on the yarn at the origin of the co-ordinate system.

(iii) The traveller is treated as a point mass.

(iv) The yarn between the traveller and the bobbin is assumed to follow a straight line path lying in the plane of the ring and tension in this portion of the yarn is assumed to be constant.

(v) Gravitational force is neglected.

(vi) Yarn is assumed to be perfectly flexible and inextensible.

(vii) Air drag force as a result of the relative velocity of air with respect to yarn along the yarn axis is assumed to be negligible. The air drag is considered significant only perpendicular to the yarn axis.

The equations of motion of the balloon in non-dimensional form have been derived[3] as:

$$-P^2R = (1 - P^2R^2/2)L^2R_{,SS} - P^2L^2RR_{,S}^2 - L^2(1-P^2R^2/2)R\Phi_{,S}^2 + Q^2L^2R^3R_{,S}\Phi_{,S}(1- L^2R^2\Phi_{,S}^2)^{1/2} \quad \ldots(1)$$

$$0 = (1 - P^2R^2/2)R_{,SS} - P^2L^2R^2R_{,S}\Phi_{,SS} - 2L^2(1-P^2R^2/2)R_{,S}\Phi_{,S} - Q^2R^2(1- L^2R^2\ \Phi_{,S}^2)3/2 \quad \ldots(2)$$

$$0 = (1 - P^2R^2/2)\ Z_{,SS} - P^2RR_{,S}Z_{,S} + Q^2R^3Z_{,S}\Phi_{,S}\ (1 - L^2R^2\ \Phi_{,S}^2)^{1/2} \quad \ldots(3)$$

where $P = M\omega^2r_o^2/T_o$; M, the mass per unit length of yarn; ω, the angular velocity of the moving frame containing the yarn segment, relative to the inertial frame; r_o, the radius of the ring; T_o, the yarn tension (T) at $r = 0$; r, the horizontal distance of the yarn segment from the balloon axis; $R = r/r_o$; $L = r_o/h$ (slenderness ratio); h, the height of balloon (vertical distance from lappet to ring); ds, the length of an infinitesimally small yarn segment of the balloon at a distance 's' from lappet (the distance is measured along the yarn axis); $S = s/h$; $R_{,s} = dR/dS$; $R_{,SS} = d^2R/dS^2$; $R_{,S}^2 = (dR/dS)^2$; $X'Y'Z'$, the moving coordinate frame with $X'Z'$ plane containing the yarn segment at the origin (i.e. the lappet); Φ, the angle between moving $X'Z'$ plane and the yarn segment ds; $Q = (D\omega^2r_o^3/T_o)^{0.5}$; D, the air drag related parameter ($C_d\rho_a d$); C_d, the coefficient of air drag; ρ_a, the density of air; d, the diameter of yarn; $Z = z/h$; and z, the vertical distance of the segment ds from the lappet.

Six boundary conditions are needed to solve the three equations [Eqs (1)-(3)]. The length of a small segment of the balloon can be expressed in polar coordinates as follows[3]:

$$dS^2 = L^2\ dR^2 + L^2\ R^2\ d\Phi^2 + dZ^2 \quad \ldots(4)$$

$R = 0$ at $s = 0$
$Z = 0$ at $s = 0$
$R = 1$ at $s = \lambda$
$Z = 1$ at $s = \lambda$

where λ is the length of yarn in the balloon.

Furthermore, RZ plane of the moving coordinate system is chosen such that

$\Phi = 0$ at $S = 0$; and $\Phi_{,S} = 0$ at $S = 0$

3.2 Solving the Equations

Attempts to solve these equations by direct methods were not successful. Symbolic equation solvers of two commercial softwares (Matlab and Maple) were also employed for this purpose but were found to be inadequate, probably because of the complexity of the equations. Thus, an attempt was made to obtain numerical solutions to these equations. Eqs (1)-(3) can be re-written as:

$$-P^2R = AL^2R'' - P^2L^2RR'^2 - L^2AR\Phi^2 + QL^2R'\Phi'B \quad \ldots(5)$$

$$0 = AR\Phi'' - R^2L^2P^2R'\Phi' + 2AR'\Phi' - B^3/(R^4Q^4) \quad \ldots(6)$$

$$0 = AZ''/L^2 - P^2RR'Z' + BZ'\Phi' \quad \ldots(7)$$

where,

$$A = (1 - P^2R^2/2)L^2 \quad \ldots(8)$$

$$B = Q^2(1 - L^2R^2\,\Phi'^2)^{0.5}R^3 \quad \ldots(9)$$

Using the condition

$dS^2 = L^2dR^2 + L^2R^2d\,\Phi^2 + dZ^2$, one can obtain the following relationships:

$$f_R = R' = (-b + \sqrt{(b^2 - 4ac)})/2a \quad \ldots(10)$$

$$f_\Phi = \Phi'' = (P^2L^2RR'\,\Phi')/A - 2R'\,\Phi'/R + B^3/(Q^4R^8) \quad \ldots(11)$$

$$f_Z = Z'' = (P^2RR'Z' - BZ'\,\Phi')/A \quad \ldots(12)$$

where,

$$a = P^2L^2R \quad \ldots(13)$$

$$b = P^2RZ'/L + 2AR\,\Phi' + P^2L^2R^3\,\Phi' - BL^2\,\Phi' \quad \ldots(14)$$

$$c = -(P^2R + A/L^2 + BZ'\,\Phi'/L^2 + B^3/(Q^4R^6) + A\,\Phi'^2 \quad \ldots(15)$$

These are of the form

$$R' = f_R(R, \Phi_2, Z_2)$$
$$Z_2' = f_Z(R, \Phi_2, Z_2)$$
$$\Phi_2' = f_\Phi(R, \Phi_2, Z_2)$$

where,

$\Phi_1 = \Phi$; $\Phi_2 = \Phi_1' = \Phi'$; $Z_1 = Z$; and $Z_2 = Z_1'$

By Euler Cauchy method[10], the following algorithms were used to solve the equations numerically:

$$R_{n+1} = R_n + \Delta S\,[f_R(R_n, \Phi_{2,n}, Z_{2,n})] \quad \ldots(16)$$

$$Z_{1,n+1} = Z_{1,n} + \Delta S\,Z_{2,n} \quad \ldots(17)$$

$$Z_{2,n+1} = Z_{2,n} + \Delta S\,[f_Z(R_n, \Phi_{2,n}, Z_{2,n})] \quad \ldots(18)$$

$$\Phi_{1,n+1} = \Phi_{1,n} + \Delta S\,\Phi_{2,n} \quad \ldots(19)$$

$$\Phi_{2,n+1} = \Phi_{2,n} + \Delta S\,[f_\Phi(R_n, \Phi_{2,n}, Z_{2,n})] \quad \ldots(20)$$

where ΔS is the step size.

After obtaining the initial values of R, Φ, Φ', Z and Z', one can get the numerical solution of the equations.

The yarn tension at the lappet (T_o) was obtained by inserting a tension measuring device just before the lappet. This allowed P and L to be obtained for all the different conditions under which yarn was spun.

For calculation of the coefficient of yarn drag (C_d), Batra *et al.*[3] have used a graph which relates C_d with Reynold's number (Re). The Reynold's number is obtained from the following relationship:

$$Re = v_m d/\eta$$

where $v_m = \omega \times r_{max}$; and η, the kinematic viscosity of air.

The r_{max} was obtained for all the 19 experiments from the images of the yarn balloon. This allows the parameter Q to be determined experimentally.

The yarn twist was 848 tpm. Hence, Δs = 1.17 mm/twist

$\Delta S = 1.17 / 140 = 0.00842$ for h = 140 mm
$\Delta S = 1.17 / 190 = 0.00615$ for h = 190 mm
$\Delta S = 1.17 / 250 = 0.00468$ for h = 250 mm

3.3 Obtaining Balloon Shape and its Validation

The yarn images captured by the camera do not show the true length of the yarn. It shows the projection of the yarn onto a vertical plane. Since yarns of two contrasting colours (red and white) were twisted, it was possible to identify lengths of 1.17 mm on the yarn balloon. Corresponding values of Z were obtained from the image. This allowed the initial values of R, Φ, Φ', Z and Z' to be determined from photographs of yarn balloon. The initial values were taken to be those at the lappet. They were then

used to solve the equation of balloon numerically by the Euler Cauchy method.[10] This gave the values of R for progressively increasing values of Z. The corresponding values of 'r' and 'z' can also be obtained. A plot of R *vs* Z would give the shape of the balloon predicted by model. The plot is shown in Fig. 1.

The same plot has been superimposed on the corresponding image of the yarn balloon in Fig. 2a. Care was taken to rescale the plot so that both the horizontal and vertical scales of the plot and the image are equal in Fig. 2a. This indicates that R = 1 corresponds to the ring radius and Z = 1 corresponds to the balloon height (from lappet to ring).

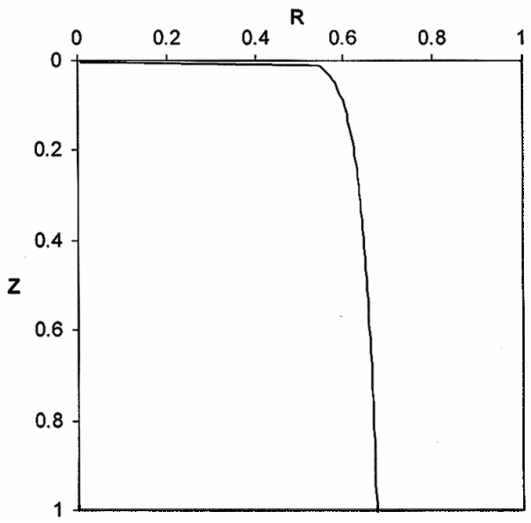

Fig. 1 — Theoretical curve of yarn balloon for h = 140 mm, 7000 rpm and 37.1mg traveller

It is observed that the balloon shape predicted by the model is quite different from the actual balloon shape. The value of 'r' is calculated to be 13.5 mm at the ring, whereas it should be 20 mm (ring radius). Similar exercises were conducted for all the spinning conditions mentioned earlier. The predicted curve was not similar in shape to the images of balloon in any of them. The error in predicting the balloon radius at the ring varies from 17mm to 6.5mm. Two more cases have been shown in Figs 2b and 2c.

Euler Cauchy method introduces truncation error in every iteration. However, the maximum truncation error was computed to be of the order of 1mm. At the ring, even the maximum error would bring the predicted curve closer to the actual image by 1mm. Round off error was negligible because all the calculations were accurate up to 14 decimal points. Use of other iterative methods for solving differential equations (e.g. Runge-Kutta method[10]) would have reduced the truncation error but would not have changed the shape of the curve.

The inability of the model to predict the balloon shape comes as a surprise, giving the results reported by Batra *et al.*[4], Zhu *et al.*[6] and Sharma and Rahn[7]. The experimental method suggested here for determining the initial conditions can be refined further. Images captured at a higher pixel depth will be able to capture the shape of the yarn balloon with

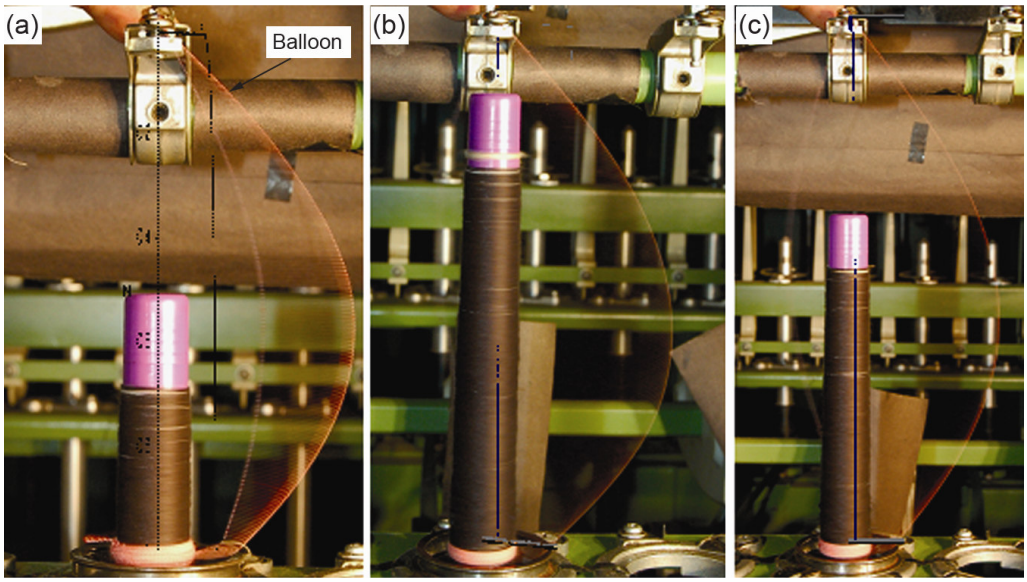

Fig. 2 — Theoretical curve of yarn balloon superimposed on balloon image for (a) h = 140 mm, 7000 rpm, 37.1 mg traveller; (b) h = 190 mm, 16000 rpm, 27.8 mg traveller; and (c) h = 250 mm, 12000 rpm, 37.1 mg traveller

greater accuracy. This will reduce the error in determining the initial conditions. Other methods of solving the equations can also be investigated. Changing the algorithm used for solving the equations from Euler Cauchy to Runge Kutta will not bring any noticeable improvement since both these will be able to satisfy only the boundary conditions at the lappet. Simultaneously satisfying the boundary conditions both at the lappet and at the traveller will require a different approach for solving the equations.

The equation of motion of the balloon has been derived with the assumption that the upper tip of the balloon does not deviate from its position. In the ring frame, this can be satisfied only by making the lappet diameter equal to the yarn diameter. In reality, the lappet diameter is 4mm while the yarn diameter is about 0.3 mm. This may result in a significant deviation of the actual balloon shape from that predicted by the equations at the lappet. Thus, the initial conditions which were measured at the lappet may have introduced large enough errors to make rest of the predicted curve significantly different from the actual balloon. A modified ring frame like experimental setup (similar to that described by Sharma and Rahn[7]) may be designed in future which will reduce or eliminate this error.

4 Conclusions

Out of the 27 different spinning conditions used, nineteen result in stable balloons. The images of these balloon envelopes have been captured by camera and then superimposed on the balloon shape predicted by the model. The difference between actual and predicted positions of the yarn at the ring varies between 6.5 mm and 17 mm for a ring radius of 20 mm. The shape of the predicted balloon is found to be quite different from the actual balloon. Better image capturing techniques and a different experimental set-up would be used to reduce the error in measurement of the initial conditions from yarn images.

Industrial Importance: A reliable method of evaluating models of yarn balloon formed during ring spinning would allow the best model to be identified. This can then be used to predict the balloon shape under widely different spinning conditions. This will allow better balloon control measures (e.g. better positioning of balloon control ring) to be adopted, resulting in an increase in spindle speed in ring frame.

References

1 DeBarr A E & Catling H, *The Principles and Theory of Ring Spinning, Manual of Cotton Spinning*, Vol. 5 (Butterworth Press, London), 1965.
2 Batra S K, Ghosh T K & Zeidman M I, *Text Res J*, 59 (6) (1989) 309.
3 Batra S K, Ghosh T K & Zeidman M I, *Text Res J*, 59 (6) (1989) 416.
4 Batra S K, Ghosh T K, Zeng Q, Robert K Q (Jr.) & Fraser W B, *Text Res J*, 65 (7), (1995) 417.
5 Ghosh T K, Batra S K, Zeidman M I & Dua B, *Text Prax Int,* 47 (September) (1992) 791, Eng XIV.
6 Zhu F, Hall K & Rahn C D, *Int J Nonlinear Mechanics*, 33 (1) (1998) 33.
7 Sharma R & Rahn C D, *J Text Inst*, 89 (1/4) (1998) 621.
8 Golubitsky M & Schaeffer D G, *Singularities and Groups in Bifurcation Theory* (Springer-Verlag, NY), 1985.
9 Perkins N C & Mote C D, *J Sound Vibration*, 114 (2) (1987) 325.
10 Kreyszig E, *Advanced Engineering Mathematics* (Wiley Eastern Ltd., New Delhi, India), 1993.